

# Excellence in Chemistry Research

## Announcing our new flagship journal

- Gold Open Access
- Publishing charges waived
- Preprints welcome
- Edited by active scientists



## Meet the Editors of *ChemistryEurope*



**Luisa De Cola**

Università degli Studi  
di Milano Statale, Italy



**Ive Hermans**

University of  
Wisconsin-Madison, USA



**Ken Tanaka**

Tokyo Institute of  
Technology, Japan

# Enhancing Dual-State Emission in Maleimide Fluorophores through Fluorocarbon Functionalisation

Maria Pervez,<sup>[a]</sup> Amanda K. Pearce,<sup>[a]</sup> Jonathan T. Husband,<sup>[a]</sup> Louise Male,<sup>[a]</sup> Miquel Torrent-Sucarrat,<sup>[b, c]</sup> and Rachel K. O'Reilly<sup>\*,[a]</sup>

**Abstract:** Herein, a library of trifluoroethyl substituted amino-maleimide derivatives are reported with small size and enhanced emissions in both solution and solid-state. A diCH<sub>2</sub>CF<sub>3</sub> substituted aminochloromaleimide exhibits the most efficient dual-state emission ( $\Phi_f > 50\%$  in solution and solid-state), with reduced quenching from protic solvents. This is attributed to the reduction of electron density on the

maleimide ring and suppressed  $\pi$ - $\pi$  stacking in the solid-state. This mechanism was explored in-depth by crystallographic analysis, and modelling of the electronic distribution of HOMO-LUMO isosurfaces and NCI plots. Hence, these dual-state dyes overcome the limitations of single-state luminescence and will serve as an important step forward for this rapidly developing nascent field.

## Introduction

Organic fluorescent materials have attracted increasing attention over the last two decades, both in academia and industry, due to their potential applications in photonics,<sup>[1]</sup> optoelectronics,<sup>[2]</sup> chemosensors,<sup>[3]</sup> and labelling.<sup>[4]</sup> Traditional organic luminophores, generally comprised of planar aromatic rings and conjugated subunits, show efficient emission in solutions but undergo quenching due to aggregate formation. This phenomenon is referred to as aggregation-caused quenching (ACQ) and limits the use of these luminophores for practical applications.<sup>[5]</sup> In 2001 another phenomenon, aggregation-induced emission (AIE), was introduced when Tang and co-workers found a series of silole derivatives that were non-emissive in dilute solutions but became highly luminescent upon aggregation, owing to the twisted propeller-shaped structures of the dye.<sup>[6]</sup> Since then, various AIE molecules with twisted shapes have been designed by suppressing intramolecular interactions and  $\pi$ - $\pi$  stacking.<sup>[7]</sup>

In the past decade, fluorophores have been developed that are emissive in both solution and solid-states, outperforming traditional fluorophores for applications such as bioimaging, optoelectronics, chiral recognition, and chemo/biosensors,<sup>[8]</sup> thus filling the gap between ACQ and AIE. However, in comparison to ACQ and AIE dyes, only a few studies on the design of dual-state emission (DSE) molecules have been reported to date. A widely employed strategy is to introduce twisted molecular conformations into the fluorophore structure, as the torsion angle between conjugated aromatic rings plays a vital role in the DSE properties.<sup>[9]</sup> Further approaches including implementing donor-acceptor structures<sup>[10]</sup> and appending long flexible alkyl chains or bulky groups<sup>[11]</sup> have also been reported to develop DSE luminophores by suppressing intramolecular interactions. Beyond these, further studies have been reported such as conjugation-induced rigidity (CIR),<sup>[12]</sup> and smart lanthanide bio-probes,<sup>[13]</sup> which are large complex structures that can be used in complex bioassay systems<sup>[14]</sup> to incorporate dual-state photoluminescence into the molecules. However, there is a major limitation in the DSE field in that reported examples typically require complex synthetic methodologies and involve large aromatic molecular frameworks. Therefore, despite the rapid development thus far, there remains an urgent need to design small and relatively simpler fluorophores, encouraging researchers to expedite the construction of dyes that are emissive in both solution and solid-states. Moreover, very few studies have focused on elucidating the mechanism of fluorescence behaviours of DSE dyes, and thus further investigation is required in this area.<sup>[15]</sup>

Small molecule organic fluorescent probes show potential in this area. In particular, maleimides are small-sized, non-invasive organic fluorophores with facile structural modification,<sup>[16]</sup> high sensitivity, and good responsivity to the physical nature of their environment.<sup>[17]</sup> Hence, they are widely applicable for the optical imaging of targets, having the virtues of structural tunability, decent cell permeability, and low cytotoxicity,<sup>[18]</sup> and as such serve as promising candidates for

[a] M. Pervez, Dr. A. K. Pearce, Dr. J. T. Husband, Dr. L. Male, Prof. R. K. O'Reilly  
School of Chemistry, University of Birmingham  
Edgbaston, Birmingham, B15 2TT (United Kingdom)  
E-mail: r.oreilly@bham.ac.uk

[b] Dr. M. Torrent-Sucarrat  
Department of Organic Chemistry I, Universidad del País Vasco (UPV/EHU)  
and Donostia International Physics Center (DIPC)  
Manuel Lardizabal Ibilbidea 3, Donostia 20018 (Spain)

[c] Dr. M. Torrent-Sucarrat  
Ikerbasque, Basque Foundation for Science  
Plaza Euskadi, 5, Bilbao 48009 (Spain)

Supporting information for this article is available on the WWW under  
<https://doi.org/10.1002/chem.202201877>

© 2022 The Authors. Chemistry - A European Journal published by Wiley-VCH GmbH. This is an open access article under the terms of the Creative Commons Attribution Non-Commercial License, which permits use, distribution and reproduction in any medium, provided the original work is properly cited and is not used for commercial purposes.

applications as biological<sup>[19]</sup> and chemical sensors.<sup>[20,21]</sup> Unsubstituted maleimides behave as fluorescence quenchers due to non-radiative excitation decay through  $n-\pi^*$  transitions<sup>[22]</sup> or photoinduced electron transfer (PET).<sup>[23]</sup> while functionalisation with amines, alcohols, or thiols turns them into powerful fluorescent probes.<sup>[16,24]</sup> This is due to the small charge differences between C=C carbons atoms, resulted from the rational introduction of electron donating and electron withdrawing groups to the maleimide motif, thus reinforcing the push-pull model.<sup>[25]</sup> Moreover, these dyes exhibit great environmental responses with significant solvatochromic effects caused by the large dipole moment change upon excitation. Unfortunately, this effect is more pronounced in polar solvents, and leads to the quenching of fluorescence as a result of electron driven proton transfer (EDPT) from protic solvents to maleimide fluorophores, which remains a major concern to be overcome.<sup>[26]</sup>

Previous research in our group has shown that thiol-substitution<sup>[27]</sup> or amino-substitution<sup>[17]</sup> to the C=C bond of the maleimide ring results in the formation of bright emissive ACQ fluorophores. It was reported that addition of an electron-donating group on the imide ring increases the emission.<sup>[28]</sup> Moreover, introducing more electron-withdrawing halogens adjacent to the electron donor group resulted in an increase in quantum yield due to lower electron density on the donor nitrogen atom.<sup>[25]</sup> Introducing an aromatic thiol adjacent to the donor amine group in a di-substituted maleimide fluorophore resulted in weak DSE contributed by the twisted conformation of a benzene ring.<sup>[25]</sup> However, despite these efforts to achieve higher emission wavelengths and brighter fluorophores, the phenomenon of fluorescence quenching continues to be problematic, and high universal emission is yet to be realised. This is either due to intermolecular interactions, which limit high emission in the solid-state as a result of ACQ, or hydrogen bonding between protic solvents and the C=O group in maleimides, thus restricting their suitability as fluorophores in polar environments.

Considering the typical electron donor-acceptor mechanism in maleimide-based fluorophores, where the C=O groups and the group on the C=C moiety act as the electron acceptor and donor respectively, it was hypothesised that the incorporation of fluorine atoms to the maleimide ring could result in enhanced fluorescence in different solvents towards optimal dual-state emission (DSE). The incorporation of these electron-withdrawing groups was expected to lower the electron density on the maleimide ring, which has previously been reported to enhance emission and reduce interactions between the carbonyl (C=O) of the maleimide ring and protic solvents, reducing EDPT. Therefore, fluorine-containing aminochloromaleimide (ACM) and monoaminomaleimide (MAM) derivatives were targeted in this work, as thus far they are the brightest known maleimide dyes<sup>[25]</sup> and are more widely reported and better understood.<sup>[29]</sup> The effect of adding a  $\text{CH}_2\text{CF}_3$  group at different positions of the maleimide ring on the resultant optical properties was explored both in solution and in the solid-state.

## Results and Discussion

A series of monoaminomaleimide (MAM) and aminochloromaleimide (ACM) dyes with  $\text{CH}_2\text{CF}_3$  groups attached at the amine and/or imide positions were synthesised starting from the appropriate anhydride (Figure 1). Dyes with different functional groups on the amine and imide positions were synthesised in a two-step process (Figure 1a, route I), while dyes bearing identical substituents at these positions could be conveniently synthesised in a single step (Figure 1a, route II). Control dyes lacking the  $\text{CF}_3$  groups (Et-ACM and Et-MAM) were synthesised for comparative purposes using the same method.

In order to understand the effect of introducing fluorine to different positions on the maleimide ring, optical properties were investigated for the three ACM compounds containing the  $\text{CH}_2\text{CF}_3$  substituent ( $\text{CF}_3$ -ACMa,  $\text{CF}_3$ -ACMb, and  $\text{diCF}_3$ -ACM) and one control (Et-ACM), using a range of solvents with different polarities (Figure 2 and Table S1).  $\text{diCF}_3$ -ACM showed an obvious red shift in absorption ( $\lambda_{\text{ab}} = 352$  to 367 nm) and emission peaks ( $\lambda_{\text{em}} = 461$  to 503 nm) when moving from a nonpolar solvent (diethyl ether) to a polar solvent (methanol), which was attributed to stabilisation of the excited state in polar environments, and thus correlated with the trend observed for non-fluorine systems as reported previously.<sup>[17,25]</sup> To quantify emission, the fluorescence quantum yields ( $\Phi_f$ ) were measured, using quinine sulfate (59%, 0.105 M  $\text{HClO}_4$ ) as

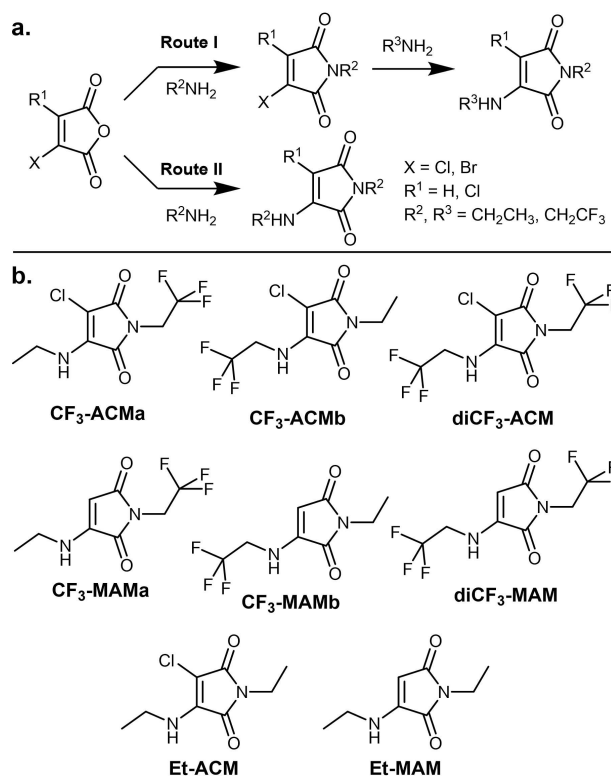


**Figure 1.** a) Synthetic routes for the dye series using an anhydride precursor. To generate the maleimide derivatives with different groups at  $\text{R}^2$  and  $\text{R}^3$  positions, route I was followed. For identical groups at  $\text{R}^2$  and  $\text{R}^3$ , route II was followed, and b) the resultant ACM and MAM library investigated in this study.

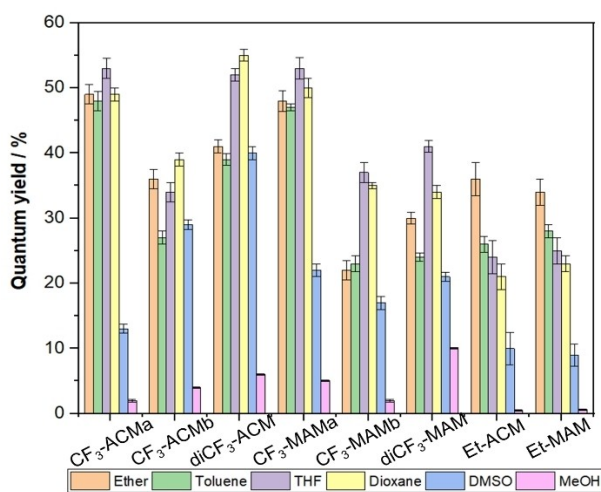


**Figure 2.** Solution-state quantum yields for the series of dyes in a range of different solvents, calculated via a reference method.<sup>[30]</sup> (10  $\mu$ M; slit widths: 1.0 nm, 1.0 nm).

reference.<sup>[30]</sup> On moving from an aprotic solvent dioxane (55%) to a protic solvent methanol (6%), a decrease in quantum yield is observed along with a longer fluorescence lifetime (compound diCF<sub>3</sub>-ACM 2.32 ns v/s Et-ACM 0.48 ns; Figure S18). Notably, whilst low, this is the highest  $\Phi_f$  of a substituted maleimide (ACM) recorded in a protic polar solvent – for example Et-ACM exhibits a  $\Phi_f$  of <1% in methanol (Figure 2). In addition, the single CH<sub>2</sub>CF<sub>3</sub> substituted ACMS, CF<sub>3</sub>-ACMa and CF<sub>3</sub>-ACMb, exhibited lower fluorescence efficiencies in comparison to the diCF<sub>3</sub>-ACM in all the solvents. The higher  $\Phi_f$  recorded for diCH<sub>2</sub>CF<sub>3</sub> substituted ACMS and MAMs than their respective single substituted ACMS/MAMs is in agreement with a decrease in electron density on the maleimide ring, as a result of electron withdrawal into the CF<sub>3</sub> groups, which is discussed further below.

Additionally, on comparing CF<sub>3</sub>-ACMa (an imide substituted CH<sub>2</sub>CF<sub>3</sub>) and CF<sub>3</sub>-ACMb (an amine substituted CH<sub>2</sub>CF<sub>3</sub>), CF<sub>3</sub>-ACMb exhibited lower  $\Phi_f$ , particularly in non-polar solvents. This corresponds to lower electron densities modelled and is also explained below (see Supporting Information, for more details). This suggests that the trifluoroethyl group (CH<sub>2</sub>CF<sub>3</sub>) has a greater electron withdrawing effect when directly linked to the imide nitrogen instead of the amino position, eventually contributing to higher emissions in the polar solvents.

Though all the fluorinated maleimide derivatives and their non-fluorinated controls displayed a similar trend in fluorescent emission across the solvent series, the MAMs yielded slightly lower emissions relative to their respective ACMS (e.g. the diCF<sub>3</sub> dye drops from around 55% in dioxane for the ACM to around 35% for the MAM) (Figure 2 and Table S1). This is due to the electron withdrawing nature of the chlorine atom reducing the electron density on the maleimide ring, in accordance with work previously reported by our group.<sup>[25]</sup>

To investigate the potential for DSE, the solid-state  $\Phi_f$  of the series were measured using an integrating sphere set-up. The

compounds diCF<sub>3</sub>-ACM and diCF<sub>3</sub>-MAM exhibited the highest solid-state  $\Phi_f$  (53% and 49%, respectively), but all the single CH<sub>2</sub>CF<sub>3</sub>-substituted ACMS/MAMs showed increased solid-state  $\Phi_f$  compared to the non-fluorinated aminomaleimides, ranging from 12–36% (Figure 3). These results reflect the trend observed for the solution-state experiments conducted in methanol, emphasising the significance of the attached CF<sub>3</sub> groups for achieving efficient DSE.

We next sought to rule out the possibility that the higher fluorescence efficiencies exhibited by trifluoroethyl maleimide derivatives in polar solvents (e.g. methanol) were caused by aggregation, resulting from the increased hydrophobicity of the added CH<sub>2</sub>CF<sub>3</sub> substituents. To explore this, emission spectra for diCF<sub>3</sub>-ACM in methanol and solid-state were compared. We observed that the emission spectra were completely different in the solid-state compared to MeOH. When aggregated, this compound generated an emission maximum around 475 nm, but was red-shifted in methanol (503 nm), signifying that the fluorophore was soluble in methanol (Figure 4). This suggests that the quantum efficiency observed in methanol is due to the dissolved species and not as a result of aggregation.

We further attempted to force aggregation to occur by investigating the emission behaviour of diCF<sub>3</sub>-ACM in mixtures of methanol with progressively larger fractions of water ( $f_w$ ). A weak emission peak at 503 nm was observed in pure methanol solution. As  $f_w$  increased from 10–40%, a decrease in intensity and a slight red shift of the emission were observed (Figure S17a). In the case of intramolecular charge transfer fluorophores, such as maleimides, excitation leads to the formation of a charge separated ground state (HOMO) and excited state (LUMO). In order to reduce the coulombic interactions the molecule may rotate, generating a twisted intramolecular charge transfer state (TICT), leading to the fluorescence quenching.<sup>[29]</sup> The solvent molecules tend to stabilize these charge states, and this effect is more pronounced with an increase in the polarity of the solvent.<sup>[31]</sup> Accordingly, a decrease in fluorescence intensity with the increase of water

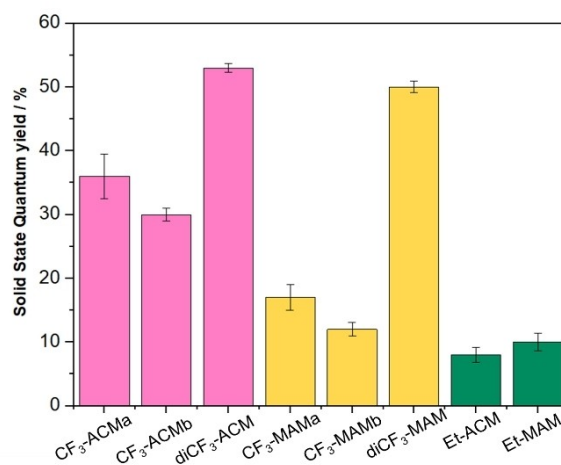


**Figure 3.** Solid-state quantum yields for the dye series, measured by an absolute method using an integrating sphere.<sup>[30]</sup>

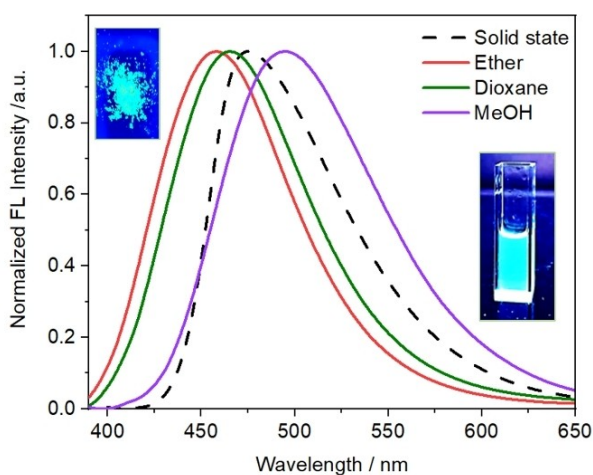


**Figure 4.** Normalized emission spectra and (inset images under UV-light in dioxane and in solid-state) of diCF<sub>3</sub>-ACM in solvents of different polarities and in solid-state (10 μM; slit widths: 1.0 nm, 1.0 nm).

content was observed. When  $f_w$  reached 40% a slight blue shift (514 to 510 nm) was observed, which was attributed to the onset of aggregation (Figure S17b). This observation further supported the full dissolution of the fluorinated dye in methanol, and therefore that dual-state emission behaviour was being exhibited.

To further investigate the origins of the unexpected high solid-state fluorescence efficiencies, single-crystal structures were obtained for the fluorinated ACMs (CF<sub>3</sub>-ACMa, CF<sub>3</sub>-ACMb, and diCF<sub>3</sub>-ACM), fluorinated MAMs (CF<sub>3</sub>-MAMa and diCF<sub>3</sub>-MAM), and Et-ACM (control). Unfortunately, the dyes CF<sub>3</sub>-MAMb and Et-MAM didn't crystallise due to their amorphous nature and therefore were unable to be compared with the other members of the series. From the molecular packing, it was observed that CF<sub>3</sub>-MAMa and Et-ACM formed dimers connected by N–H...O bonds, while for CF<sub>3</sub>-ACMa and CF<sub>3</sub>-ACMb relatively open structures were observed, which was attributed to the twisted, propeller-like arrangement of CF<sub>3</sub> (Figure 5, Figure S20–24). The molecules were alternately arranged up and down and formed parallel layers through N–H...O interactions 2.09 to 2.16 Å long (Table S2). In the case of CF<sub>3</sub>-MAMa, it is noteworthy that dimers were connected by weak C–H...O interactions which were absent in the ACM fluorophores. Additionally, intermolecular  $\pi$ - $\pi$  stacking between the parallel layers led to a  $\pi$ - $\pi$ -packed zigzag arrangement (Figure S20–24). We propose that the high solid-state emission can be explained by these more distant  $\pi$ - $\pi$  interactions: we have reported how  $\pi$ - $\pi$  stacking interactions result in fluorescence quenching of the dyes.<sup>[32]</sup> To quantify this, we evaluated inter-ring centroid distances, and it was observed that the ring spacings are consistent with  $\pi$ - $\pi$  stacking interactions. Higher inter-ring centroid distances observed for the fluorinated dyes > 4 Å correlated with higher solid-state  $\Phi_f$  (Figure S19 and Table S3). The control EtACM, with the shortest observed ring centroid distance i.e. 3.69 Å gave the lowest solid-state  $\Phi_f$ . This can be most likely explained as the result of intermolecular quenching interactions, and was also further

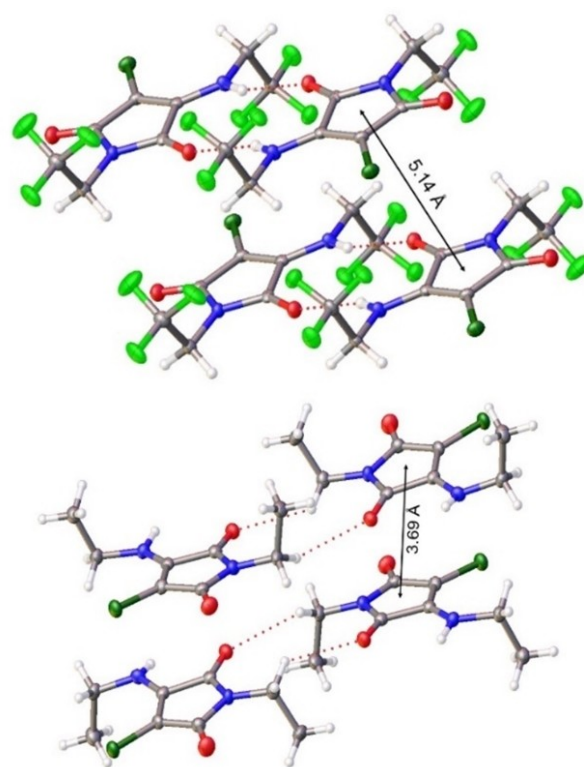


**Figure 5.** Molecular alignments of diCF<sub>3</sub>-ACM (top) and Et-ACM (bottom) in a single crystal.

envisaged by the visualisation of the noncovalent interactions. The observed molecular conformations of the fluorinated dyes in the crystals owing to the intermolecular interactions block the non-radiative relaxation,<sup>[33]</sup> which contributes to their high solid-state  $\Phi_f$  (Table S3).

Finally, to gain further insights into the origin of the efficient dual-state emission of the CH<sub>2</sub>CF<sub>3</sub>-functionalised maleimide derivatives, time-dependent density functional theory calculations were performed. The lowest-energy absorption and emission peaks were computed at CAM-B3LYP-GD3BJ(PCM)/6-311G(d,p) level (see Supporting Information for more details). A good agreement between the theoretical and experimental values was obtained. All excitation and emission energies correspond to the first excited state ( $\pi$ - $\pi^*$  and  $\pi^*$ - $\pi$  transitions, respectively).

Additionally, a thorough analysis of the natural population charges was performed to quantify the electron redistribution of the different substituents in the aminomaleimide derivative rings. The higher fluorescence efficiency in methanol is attributed to the presence of the fluorine substituents (CH<sub>2</sub>CF<sub>3</sub>) reducing the electron density on the C=O bonds, decreasing their ability to abstract solvent protons, and therefore undergo EDPT. The effect of the position of the trifluoroethyl group on the maleimide ring is thus shown to be vital. Its position in CF<sub>3</sub>-ACMa, with the CH<sub>2</sub>CF<sub>3</sub> group attached to the imide position, offers a more important electron withdrawing effect than CF<sub>3</sub>-ACMb when the CH<sub>2</sub>CF<sub>3</sub> is attached to the amine position.

Further, higher  $\Phi_f$  (%) for the di-CH<sub>2</sub>CF<sub>3</sub> substituted ACM and MAM than their respective single-CH<sub>2</sub>CF<sub>3</sub> substituted ACM/MAM agrees with the reduction of the electron density in the aminomaleimide ring. Finally, the visualisation of the non-covalent interaction descriptor allows for validation of the  $\pi$ - $\pi$  interactions hypothesised in the crystal data (Figure S20–24).

## Conclusion

Rational substitution of MAMs and ACMs with trifluoroethyl groups has allowed us to tune electron density on the maleimide dye core, helping realise increased fluorescence efficiency in the solution and solid-state. The enhanced solution-state  $\Phi_f$  in protic solvents (up to 6–10%) was explained through the withdrawal of electron density away from carbonyl quenching interactions and into the trifluoroethyl groups. In addition, enhanced solid-state  $\Phi_f$  emission (up to 53%) was achieved through the steric hindrance of the trifluoroethyl groups, reducing the quenching induced by the intermolecular interactions; for example  $\pi$ - $\pi$  stacking. These advances make these compounds great candidates for dual-state emission applications. It is envisioned these will be powerful in various biochemical and materials applications, where dyes with efficient dual-state emission, small size, and neutral polarity are needed.

## Experimental Section

Detailed information on general procedures, computational details and results, product characterisation, and fluorescence analysis can be found in the Supporting Information.

Deposition Numbers 2161051–2161056 contain the supplementary crystallographic data for this paper. These data are provided free of charge by the joint Cambridge Crystallographic Data Centre and Fachinformationszentrum Karlsruhe Access Structures service [www.ccdc.cam.ac.uk/structures](http://www.ccdc.cam.ac.uk/structures).

## Acknowledgements

The authors thank the Ministerio de Economía y Competitividad (MINECO) of Spain (project: PID2019-104772GB-I00) and the Basque Government (project IT1346-19), and the Leverhulme Trust (RPG-2016-452). Dr. Thomas R. Wilks and Dr. Yujie Xie are thanked for helpful discussions and Chi Tsang (University of Birmingham) for high resolution mass spectroscopy analysis. The authors acknowledge the computational resources, and technical and human support provided by the DIPC.

## Conflict of Interest

The authors declare no conflict of interest.

## Data Availability Statement

The data that support the findings of this study are available from the corresponding author upon reasonable request.

**Keywords:** aminochloromaleimide · dual-state emission · fluorocarbons · maleimide fluorophores · monoaminomaleimide

- [1] J. L. Brennan, T. E. Keyes, R. J. Forster, *Langmuir* **2006**, *22*, 10754–10761.
- [2] L. Zhu, Y. Zhao, *J. Mater. Chem. C* **2013**, *1*, 1059–1065.
- [3] D. Wu, A. C. Sedgwick, T. Gunnlaugsson, E. U. Akkaya, J. Yoon, T. D. James, *Chem. Soc. Rev.* **2017**, *46*, 7105–7123.
- [4] T. Terai, T. Nagano, *Curr. Opin. Chem. Biol.* **2008**, *12*, 515–521.
- [5] a) Y. Chen, J. W. Y. Lam, R. T. K. Kwok, B. Liu, B. Z. Tang, *Mater. Horiz.* **2019**, *6*, 428–433; b) N. S. S. Kumar, M. D. Gujrati, J. N. Wilson, *Chem. Commun.* **2010**, *46*, 5464–5466.
- [6] J. Luo, Z. Xie, J. W. Y. Lam, L. Cheng, H. Chen, C. Qiu, H. S. Kwok, X. Zhan, Y. Liu, D. Zhu, B. Z. Tang, *Chem. Commun.* **2001**, 1740–1741.
- [7] a) Z. Lou, Y. Hou, K. Chen, J. Zhao, S. Ji, F. Zhong, Y. Dede, B. Dick, *J. Phys. Chem. C* **2018**, *122*, 185–193; b) Z. Peng, Y. Ji, Z. Huang, B. Tong, J. Shi, Y. Dong, *Mater. Chem. Front.* **2018**, *2*, 1175–1183; c) Y. Yang, X. Wang, Q. Cui, Q. Cao, L. Li, *ACS Appl. Mater. Interfaces* **2016**, *8*, 7440–7448.
- [8] a) Y. Liu, Y. Zhang, X. Wu, Q. Lan, C. Chen, S. Liu, Z. Chi, L. Jiang, X. Chen, J. Xu, *J. Mater. Chem. C* **2014**, *2*, 1068–1075; b) H. Liu, Q. Bai, L. Yao, H. Zhang, H. Xu, S. Zhang, W. Li, Y. Gao, J. Li, P. Lu, H. Wang, B. Yang, Y. Ma, *Chem. Sci.* **2015**, *6*, 3797–3804.
- [9] a) X. Zhang, Y. Zhou, M. Wang, Y. Chen, Y. Zhou, W. Gao, M. Liu, X. Huang, H. Wu, *Chem. Asian J.* **2020**, *15*, 1692–1700; b) J. Price, E. Albright, A. Decken, S. Eisler, *Org. Biomol. Chem.* **2019**, *17*, 9562–9566; c) K. Ramamurthy, E. J. P. Malar, C. Selvaraju, *New J. Chem.* **2019**, *43*, 9090–9105.
- [10] a) Q. Qiu, P. Xu, Y. Zhu, J. Yu, M. Wei, W. Xi, H. Feng, J. Chen, Z. Qian, *Chem. Eur. J.* **2019**, *25*, 15983–15987; b) N. Jian, K. Qu, H. Gu, L. Zou, X. Liu, F. Hu, J. Xu, Y. Yu, B. Lu, *Phys. Chem. Chem. Phys.* **2019**, *21*, 7174–7182; c) V. D. Singh, A. K. Kushwaha, R. S. Singh, *Dyes Pigm.* **2021**, *187*, 109117.
- [11] a) Y. Xu, L. Ren, D. Dang, Y. Zhi, X. Wang, L. Meng, *Chem. Eur. J.* **2018**, *24*, 10383–10389; b) Y. Zhang, Y. Qu, J. Wu, Y. Rui, Y. Gao, Y. Wu, *Dyes Pigm.* **2020**, *179*, 108431.
- [12] a) Y. Liu, Y. Zhang, X. Wu, Q. Lan, C. Chen, S. Liu, Z. Chi, L. Jiang, X. Chen, J. Xu, *J. Mater. Chem. C* **2014**, *2*, 1068–1075; b) G. Chen, W. Li, T. Zhou, Q. Peng, D. Zhai, H. Li, W. Z. Yuan, Y. Zhang, B. Z. Tang, *Adv. Mater.* **2015**, *27*, 4496–4501.
- [13] Y. Zhang, P. C. Jiao, H. B. Xu, M. J. Tang, X. P. Yang, S. Huang, J. G. Deng, *Sci. Rep.* **2015**, *5*, 9335.
- [14] X. Zhou, H. Yang, Z. Chen, S. Gong, Z.-H. Lu, C. Yang, *J. Mater. Chem. C* **2019**, *7*, 6607–6615.
- [15] a) Y. Li, Y. Lei, L. Dong, L. Zhang, J. Zhi, J. Shi, B. Tong, Y. Dong, *Chem. Eur. J.* **2019**, *25*, 573–581; b) M. Huang, R. Yu, K. Xu, S. Ye, S. Kuang, X. Zhu, Y. Wan, *Chem. Sci.* **2016**, *7*, 4485–4491; c) J. L. Belmonte-Vázquez, Y. A. Amador-Sánchez, L. A. Rodríguez-Cortés, B. Rodríguez-Molina, *Chem. Mater.* **2021**, *33*, 7160–7184.
- [16] H.-C. Yeh, W.-C. Wu, C.-T. Chen, *Chem. Commun.* **2003**, 404–405.
- [17] A. B. Mabire, M. P. Robin, W.-D. Quan, H. Willcock, V. G. Stavros, R. K. O'Reilly, *Chem. Commun.* **2015**, *51*, 9733–9736.
- [18] H.-W. Liu, L. Chen, C. Xu, Z. Li, H. Zhang, X.-B. Zhang, W. Tan, *Chem. Soc. Rev.* **2018**, *47*, 7140–7180.
- [19] a) C. M. Grison, G. M. Burslem, J. A. Miles, L. K. A. Pils, D. J. Yeo, Z. Imani, S. L. Warriner, M. E. Webb, A. J. Wilson, *Chem. Sci.* **2017**, *8*, 5166–5171; b) E. A. Hull, M. Livanos, E. Miranda, M. E. B. Smith, K. A. Chester, J. R. Baker, *Bioconjugate Chem.* **2014**, *25*, 1395–1401.
- [20] A. M. Eissa, P. Wilson, C. Chen, J. Collins, M. Walker, D. M. Haddleton, N. R. Cameron, *Chem. Commun.* **2017**, *53*, 9789–9792.
- [21] Z. Yang, Y. Guo, S.-L. Ai, S.-X. Wang, J.-Z. Zhang, Y.-X. Zhang, Q.-C. Zou, H.-X. Wang, *Mater. Chem. Front.* **2019**, *3*, 571–578.
- [22] a) J. Guy, K. Caron, S. Dufresne, S. W. Michnick, W. G. Skene, J. W. Keillor, *J. Am. Chem. Soc.* **2007**, *129*, 11969–11977; b) Y. Kanaoka, M. Machida, K. Ando, T. Sekine, *Biochim. Biophys. Acta.* **1970**, *207*, 269–277.
- [23] A. Prasanna de Silva, H. Q. Nimal Gunaratne, T. Gunnlaugsson, *Tetrahedron Lett.* **1998**, *39*, 5077–5080.

- [24] Z. Yang, J. Cao, Y. He, J. H. Yang, T. Kim, X. Peng, J. S. Kim, *Chem. Soc. Rev.* **2014**, *43*, 4563–4601.
- [25] Y. Xie, J. T. Husband, M. Torrent-Sucarrat, H. Yang, W. Liu, R. K. O'Reilly, *Chem. Commun.* **2018**, *54*, 3339–3342.
- [26] a) M. Staniforth, W.-D. Quan, T. N. V. Karsili, L. A. Baker, R. K. O'Reilly, V. G. Stavros, *J. Phys. Chem. A* **2017**, *121*, 6357–6365; b) B. Valeur, J.-C. Brochon, *New Trends in Fluorescence Spectroscopy: Applications to Chemical and Life Sciences*, Springer-Verlag Berlin Heidelberg **2001**.
- [27] M. P. Robin, P. Wilson, A. B. Mabire, J. K. Kiviaho, J. E. Raymond, D. M. Haddleton, R. K. O'Reilly, *J. Am. Chem. Soc.* **2013**, *135*, 2875–2878.
- [28] H.-d. Xie, L. A. Ho, M. S. Truelove, B. Corry, S. G. Stewart, *J. Fluoresc.* **2010**, *20*, 1077–1085.
- [29] Q. Zhu, Z. Ye, W. Yang, X. Cai, B. Z. Tang, *J. Org. Chem.* **2017**, *82*, 1096–1104.
- [30] C. Würth, M. Grabolle, J. Pauli, M. Spieles, U. Resch-Genger, *Nat. Protoc.* **2013**, *8*, 1535–1550.
- [31] G. Haberhauer, R. Gleiter, C. Burkhart, *Chem. Eur. J.* **2016**, *22*, 971–978.
- [32] J. T. Husband, Y. Xie, T. R. Wilks, L. Male, M. Torrent-Sucarrat, V. G. Stavros, R. K. O'Reilly, *Chem. Sci.* **2021**, *12*, 10550–10557.
- [33] R. Zheng, X. Mei, Z. Lin, Y. Zhao, H. Yao, W. Lv, Q. Ling, *J. Mater. Chem. C* **2015**, *3*, 10242–10248.

---

Manuscript received: June 17, 2022

Accepted manuscript online: July 20, 2022

Version of record online: August 24, 2022